

Mesons and diquarks in Coulomb-gauge QCD

R.F. Wagenbrunn

Institut für Physik, Fachbereich Theoretische Physik,
Karl-Franzens-Universität Graz, Universitätsplatz 5, A-8010 Austria

Abstract

I demonstrate how confinement in Coulomb-gauge QCD makes quark-quark states of the color anti-triplet (diquarks) move out of the physical spectrum. Mesons as color singlet quark-antiquark states, on the other hand have finite masses and for highly excited states in the meson spectra effective restoration of chiral symmetry can be observed.

In Coulomb-gauge QCD the 00-component of the gluon propagator $D_{\mu\nu}(\vec{x}, t)$ has an instantaneous part $V_C(\vec{x})\delta(t)$ and confinement means that $-V_C(\vec{x}) \rightarrow \infty$ for $|\vec{x}| \rightarrow \infty$. It was shown that Coulomb confinement is a necessary condition for confinement, i.e., that the gauge invariant quark-antiquark potential $V_W(r)$ goes to infinity for $r \rightarrow \infty$ [1]. An almost linearly rising Coulomb potential has been suggested [2], which was also confirmed by results from the lattice [3]. In momentum space it becomes

$$V_C(|\vec{k}|) = \frac{\sigma_C}{|\vec{k}|^4}, \quad (1)$$

where σ_C is the Coulomb string tension. Based on previous works [4] we performed a study of the mechanism of Coulomb confinement in the Dyson-Schwinger–Bethe-Salpeter framework [5] in Rainbow-ladder approximation [6]. We took into account only the Coulomb potential (1) and neglected transverse gluons and noninstantaneous contributions to D_{00} . In that way all integrals over k_0 can be performed analytically and one has to deal with three-dimensional integral equations only. (1) has also an unrealistic ultraviolet (UV) behavior. However, it has the advantage that it produces no UV divergences, thus making renormalization not necessary. Due to all these approximations some physics is lost and the model is not expected to provide realistic quantitative results but some qualitative insight into the physics of confinement in QCD. Since the axial-vector Ward-Takahashi

identity is satisfied, chiral symmetry and its dynamical breaking are respected. In particular the pion mass becomes zero in the chiral limit, i.e., for vanishing current quark mass. The potential (1) causes infrared (IR) divergences which are regulated by introducing an IR regulator μ_{IR} and replacing $k^2 \rightarrow k^2 + \mu_{\text{IR}}^2$ (here and in the following $k = |\vec{k}|$). The IR limit is then taken by means of $\mu_{\text{IR}} \rightarrow 0$. The essential point is that the integral

$$\frac{1}{2\pi^2} \int d^3q \frac{1}{((\vec{p} - \vec{q})^2 + \mu_{\text{IR}}^2)^2} = \frac{1}{2\mu_{\text{IR}}} \quad (2)$$

diverges in the IR limit and one can write

$$\frac{1}{2\pi^2} \int d^3q V_C(|\vec{p} - \vec{q}|) f(q) = \frac{\sigma_C}{2\mu_{\text{IR}}} \int d^3q \delta(\vec{p} - \vec{q}) f(q) + \text{IR finite term.} \quad (3)$$

For the gap equation of the quark propagator $S(p)$ the ansatz

$$S^{-1}(p) = -i(\gamma_0 p_0 - \vec{\gamma} \cdot \vec{p} C(p) - B(p)) \quad (4)$$

leads to a coupled system of two integral equations

$$B(p) = m + \frac{1}{2\pi^2} \int d^3q V_C(|\vec{p} - \vec{q}|) \frac{M(q)}{\bar{\omega}(q)} \quad (5)$$

$$C(p) = 1 + \frac{1}{2\pi^2} \int d^3q V_C(|\vec{p} - \vec{q}|) \hat{p} \cdot \hat{q} \frac{q}{p \bar{\omega}(q)}, \quad (6)$$

where $\hat{p} = \vec{p}/p$, m is the current-quark mass, $\bar{\omega}(p) = \sqrt{M^2(p) + p^2}$ and $M(q) = \frac{B(q)}{C(q)}$ is called the quark mass function. Using (3) yields

$$B(p) = \frac{\sigma_C}{2\mu_{\text{IR}}} \frac{M(p)}{\bar{\omega}(p)} + \text{IR finite term} = \frac{\sigma_C}{2\mu_{\text{IR}}} \frac{B(p)}{\omega(p)} + \text{IR finite term}, \quad (7)$$

$$C(p) = \frac{\sigma_C}{2\mu_{\text{IR}}} \frac{1}{\bar{\omega}(p)} + \text{IR finite term} = \frac{\sigma_C}{2\mu_{\text{IR}}} \frac{C(p)}{\omega(p)} + \text{IR finite term}, \quad (8)$$

with

$$\omega(p) = \sqrt{B^2(p) + p^2 C^2(p)} = \frac{\sigma_C}{2\mu_{\text{IR}}} + \text{IR finite term.} \quad (9)$$

The functions $B(p)$ and $C(p)$ diverge like μ_{IR}^{-1} but the mass function is IR finite. The IR behavior for $M(p)$ and $\omega(p)$ for $m = 0$ is demonstrated in the upper plots of Fig. 1, while in the lower plots the same quantities for constant $\mu_{\text{IR}} = 10^{-3} \sqrt{\sigma_C}$ but different current quark masses are shown. The mass function converges to a finite function. For large p

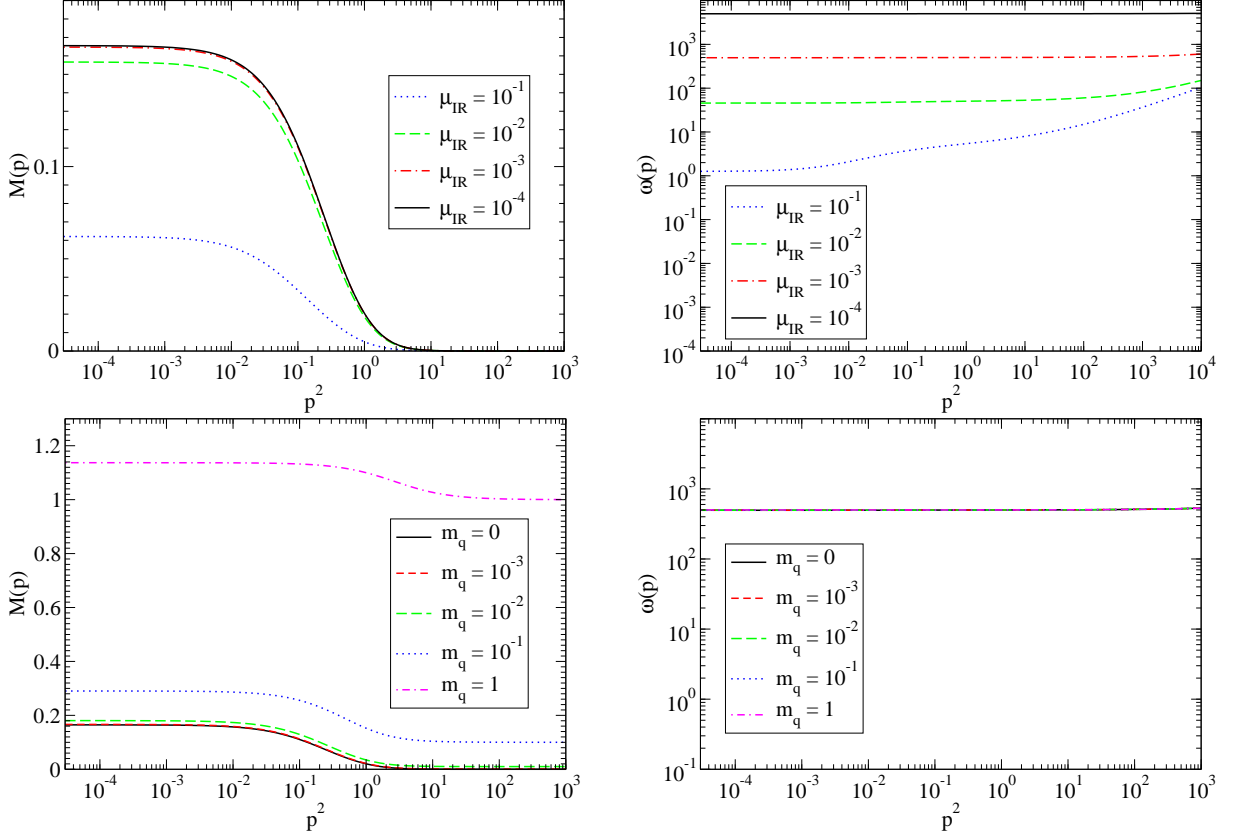


Figure 1: Mass function $M(p)$ (left plots) and $\omega(p)$ (right plots): In the upper plots the IR behavior for current quark mass $m = 0$ and in the lower plots the results for different current quark masses at constant $\mu_{\text{IR}} = 10^{-3} \sqrt{\sigma_C}$ is shown.

it goes to the current quark mass and for small p it gets a dynamical mass which is of approximately the same absolute size for different current quark masses. $\omega(p)\mu_{\text{IR}}$ indeed becomes a constant $\frac{\sigma_C}{2}$, which is independent of the current quark mass.

The Bethe-Salpeter equation (BSE) for a meson with mass M is

$$\chi(p, M) = -i \int \frac{d^4q}{(2\pi)^4} V_C(|\vec{p} - \vec{q}|) \gamma_0 S(q_0 + M/2, q) \chi(q, M) S(q_0 - M/2, q) \gamma_0. \quad (10)$$

For the pseudoscalar meson (pion with $M = m_\pi$) the Bethe-Salpeter amplitude $\chi(p, m_\pi)$ contains three (pseudoscalar, axial-vector and tensor) components:

$$\chi(p, m_\pi) = P_p(p) \gamma_5 + m_\pi P_A(p) \gamma_0 \gamma_5 + m_\pi P_T(p) \hat{p} \cdot \vec{\gamma} \gamma_0 \gamma_5. \quad (11)$$

The BSE is reduced to a coupled system of integral equations

$$\omega(p)h(p) = \frac{1}{2\pi^2} \int d^3q V_C(|\vec{p}-\vec{q}|) \left(h(q) + \frac{m_\pi^2}{4\omega(q)} g(q) \right), \quad (12)$$

$$\left(\omega(p) - \frac{m_\pi^2}{4\omega(p)} \right) g(p) = h(p) + \frac{1}{2\pi^2} \int d^3q V_C(|\vec{p}-\vec{q}|) \frac{M(p)M(q) + \vec{p} \cdot \vec{q}}{\bar{\omega}(p)\bar{\omega}(q)} g(q) \quad (13)$$

for the two functions

$$h(p) = \frac{P_p(p)}{\omega(p)}, \quad (14)$$

$$g(p) = \frac{\omega(p)}{\omega^2(p) - \frac{m_\pi^2}{4}} \left[h(p) + 2 \frac{M(p)}{\bar{\omega}(p)} P_A(p) + 2 \frac{p}{\bar{\omega}(p)} P_T(p) \right]. \quad (15)$$

The IR behavior of Eqs. (12,13) follows by using Eq. (9) on the left and Eq. (3) on the right hand sides, respectively, which yields

$$\frac{\sigma_C}{2\mu_{\text{IR}}} h(p) + \text{IR finite term} = \frac{\sigma_C}{2\mu_{\text{IR}}} h(p) + \text{IR finite term}, \quad (16)$$

$$\frac{\sigma_C}{2\mu_{\text{IR}}} g(p) + \text{IR finite term} = \frac{\sigma_C}{2\mu_{\text{IR}}} g(p) + \text{IR finite term}. \quad (17)$$

Obviously the IR divergences cancel in both equations and all physical observables, in particular the mass, are determined by the IR finite terms. The functions $h(p)$ and $g(p)$ have an IR finite limit, too. This is demonstrated for $m = 0$ in the left plot of Fig. 2.

For two quarks in the $SU(3)_C$ anti-triplet state (diquark) a color factor $\frac{1}{2}$ enters into the BSE kernel. Apart from that for a scalar diquark with mass m_{SD} one has the same integral equations as for the pion but the IR divergent terms on the right hand sides of Eqs. (16,17) are reduced to only half their sizes. Thus there must be additional IR divergences. Replacing (16,17) by

$$\frac{\sigma_C}{2\mu_{\text{IR}}} h(p) + \text{IR finite term} = \frac{\sigma_C}{4\mu_{\text{IR}}} h(p) + \frac{m_{\text{SD}}^2}{8} g(p) + \text{IR finite term}, \quad (18)$$

$$\frac{\sigma_C}{2\mu_{\text{IR}}} g(p) - \frac{m_{\text{SD}}^2 \mu_{\text{IR}}}{2\sigma_C} g(p) + \text{IR finite term} = h(p) + \frac{\sigma_C}{4\mu_{\text{IR}}} g(p) + \text{IR finite term} \quad (19)$$

and solving for m_{SD} and $g(p)$ yields

$$m_{\text{SD}} = \frac{\sigma_C}{2\mu_{\text{IR}}}, \quad g(p) = \frac{8\mu_{\text{IR}}}{\sigma_C} h(p). \quad (20)$$

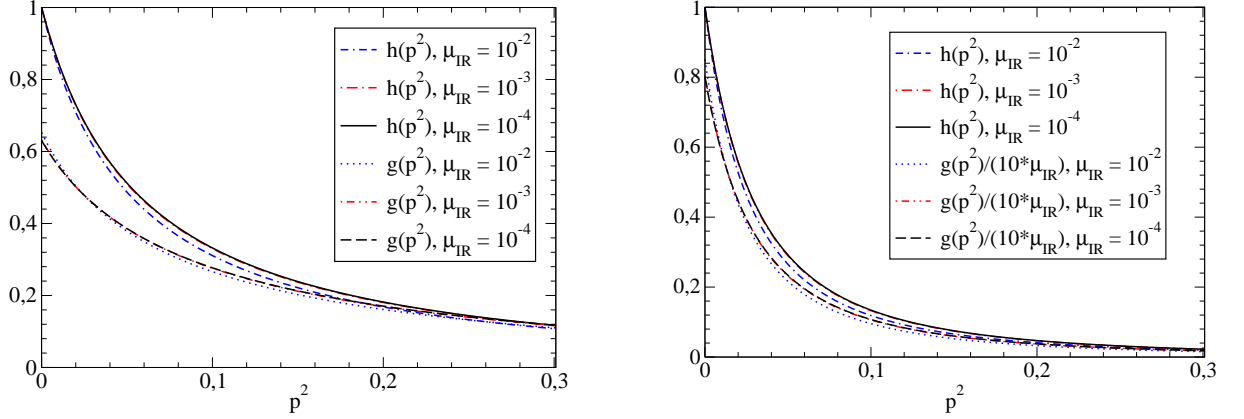


Figure 2: IR limit of the functions h and g for the pion (left) and the scalar diquark (right) for $m = 0$. In all cases the normalization has been chosen such that $h(0) = 1$.

The divergences are now balanced by introducing a relation between $h(p)$ and $g(p)$ and making the diquark mass IR divergent. In that way the diquarks are removed from the physical spectrum. This mechanism of confinement applies not only for the scalar diquark but for diquarks of all quantum numbers. Numerically we have reproduced the IR divergence of the mass for scalar and axial-vector diquarks [6]. On the other hand, the shape of the functions $h(p)$ and $g(p)$ converges in the IR limit, which is demonstrated in the right plot of Fig. 2. For that reason not only mesons but also diquarks have IR finite radii. Calculations for the electromagnetic form factor and the charge radius of the pion in Coulomb-gauge QCD have already been performed earlier [7]. Explicitly, the charge radius of the pion is given by

$$r_\pi^2 = \frac{3}{\mathcal{N}_\pi^2} \int \frac{d^3p}{(2\pi)^3} \left\{ -\frac{3}{32\bar{\omega}^4(p)} \left[2\bar{\omega}^2(p) + (M(p) - 2p^2 M'(p))^2 \right] g(p)h(p) + \frac{1}{16} [g'(p)h(p) + g(p)h'(p)] + \frac{p^2}{24} [g(p)h''(p) + g''(p)h(p) - 2g'(p)h'(p)] \right\} + \mathcal{O}(\mu_{\text{IR}}) \quad (21)$$

with

$$\mathcal{N}_\pi^2 = 3 \int \frac{d^3p}{(2\pi)^3} g(p)h(p), \quad (22)$$

and of the scalar diquark by

$$r_{\text{SD}}^2 = \frac{3\mu_{\text{IR}}}{\mathcal{N}_{\text{SD}}^2} \int \frac{d^3p}{(2\pi)^3} \left\{ -\frac{7}{6\bar{\omega}^4(p)} \left[2\bar{\omega}^2(p) + (M(p) - 2p^2 M'(p))^2 \right] h^2(p) \right\}$$

$$+2h(p)h'(p) + \frac{4p^2}{3} [h(p)h''(p) - h'^2(p)] \Big\} + \mathcal{O}(\mu_{\text{IR}}) \quad (23)$$

with

$$\mathcal{N}_{\text{SD}}^2 = 48\mu_{\text{IR}} \int \frac{d^3p}{(2\pi)^3} h^2(p). \quad (24)$$

In both cases ' means $\frac{d}{d(p^2)}$. For quark mass $m = 0$ we have obtained the results $r_\pi = 4.3 \sigma_C^{-1/2}$ and $r_{\text{SD}} = 6.0 \sigma_C^{-1/2}$ [6]. Notice that \mathcal{N}_π^2 converges to a finite value while $\mathcal{N}_{\text{SD}}^2$ goes to zero like μ_{IR} . That means that for the diquark only the shape of $h(p)$ converges but its size diverges like $\mu_{\text{IR}}^{-1/2}$. Due to (20), the size of $g(p)$ goes to zero like $\mu_{\text{IR}}^{1/2}$ on the other hand.

Finally I present results for the highly excited meson spectra in the chiral limit [8]. There are certain phenomenological evidences that in highly excited hadrons the chiral ($SU(2)_L \times SU(2)_R$) and $U(1)_A$ symmetries are approximately restored (for a review see [9]). The states fall into approximate multiplets of $SU(2)_L \times SU(2)_R$ and the mass splittings within the multiplets vanish at radial quantum number $n \rightarrow \infty$ and/or spin $J \rightarrow \infty$. Furthermore the splittings within a multiplet become much smaller than between the two subsequent multiplets. The reason for this ‘‘effective’’ symmetry restoration is that excited hadrons gradually decouple from the quark condensates due to a diminishing importance of quantum fluctuations [10]. I restrict the discussion here to scalar and pseudoscalar mesons. Given the complete set of standard quantum numbers I, J^{PC} , the multiplets of $SU(2)_L \times SU(2)_R$ for $J = 0$ are [11]

$$(1/2, 1/2)_a : 1, 0^{-+} \longleftrightarrow 0, 0^{++} \quad \text{and} \quad (1/2, 1/2)_b : 1, 0^{++} \longleftrightarrow 0, 0^{-+}.$$

The BSE for a scalar meson with mass $m_{0^{++}}$ is reduced to the coupled system of integral equations

$$h(p)\omega(p) = \frac{1}{2\pi^2} \int d^3q V_C(|\vec{p} - \vec{q}|) \frac{pq + M(p)M(q)\hat{p} \cdot \hat{q}}{\bar{\omega}(p)\bar{\omega}(q)} \left(h(q) + \frac{m_{0^{++}}^2}{4\omega(q)} g(q) \right), \quad (25)$$

$$g(p) \left(\omega(p) - \frac{m_{0^{++}}^2}{4\omega(p)} \right) = h(p) + \frac{1}{2\pi^2} \int d^3q V_C(|\vec{p} - \vec{q}|) \hat{p} \cdot \hat{q} g(q). \quad (26)$$

For highly excited states the typical momenta of the quarks become large. For large momenta, however, the mass function $M(p)$ becomes small. Setting $M(p) = 0$ in the second equation for the pseudoscalar meson (13) and the first equation for the scalar meson (25) gives just the second equation for the scalar meson (26) and the first equation for the pseudoscalar meson (12), respectively. For large momenta with $M(p) \approx 0$ the two

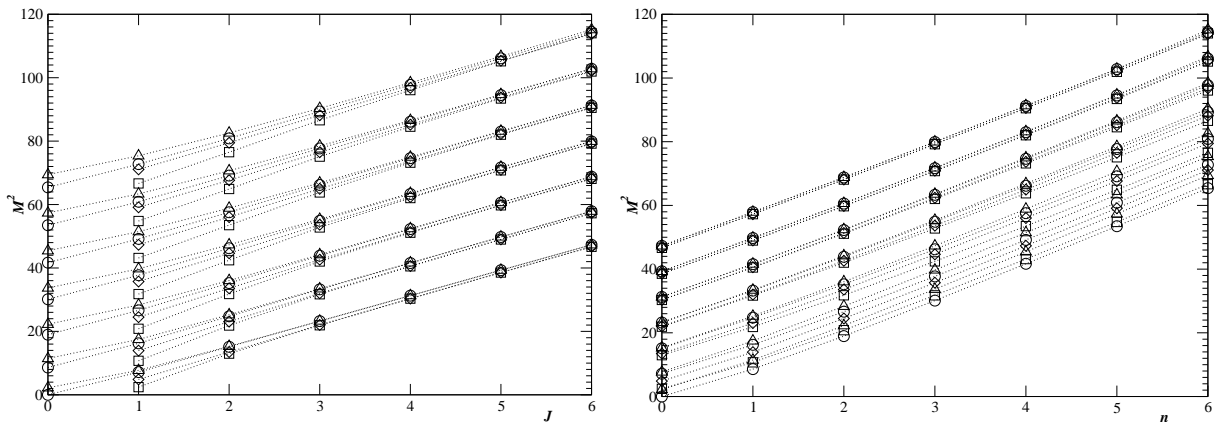


Figure 3: Angular (left) and radial (right) Regge trajectories for isovector mesons. Mesons of the chiral multiplet $(1/2, 1/2)_a$ are indicated by circles, of $(1/2, 1/2)_b$ by triangles, and of $(0, 1) \oplus (1, 0)$ by squares (J^{++} and J^{--} for even and odd J , respectively) and diamonds (J^{--} and J^{++} for even and odd J , respectively).

systems of coupled integral equations become approximately the same. This can explain why pseudoscalar and scalar mesons with large n become approximately degenerate. For states with $J > 0$ similar arguments hold but there are additional states which fall in the multiplets $(0, 0)$ and $(0, 1) \oplus (1, 0)$. The Bethe-Salpeter amplitudes for mesons with large J become strongly suppressed for small momenta and already states with $n = 0$ become approximately degenerate. In our model the numerical results for the meson spectra up to $n, J = 6$ show a very fast restoration of both $SU(2)_L \times SU(2)_R$ and $U(1)_A$ symmetries with increasing J and essentially more slow restoration with increasing n . The excited states lie on approximately linear radial and angular Regge trajectories which is demonstrated in Fig. 3. In the limit $n \rightarrow \infty$ and/or $J \rightarrow \infty$ one observes an approximate degeneracy of all states within the representation $[(0, 1/2) \oplus (1/2, 0)] \times [(0, 1/2) \oplus (1/2, 0)]$ that combines all possible chiral representations for systems of two massless quarks [11].

Acknowledgment: The results presented in this contribution were obtained in collaboration with R. Alkofer, L. Ya. Glozman, M. Kloker, and A. Krassnigg. I am grateful to the organizers for providing financial support for my participation at the workshop.

References

- [1] D. Zwanziger, Phys. Rev. Lett. **90**, 102001 (2003).

- [2] A. P. Szczepaniak and E. S. Swanson, Phys. Rev. D **65**, 025012 (2002); D. Zwanziger, Phys. Rev. D **70**, 094034 (2004); C. Feuchter and H. Reinhardt, Phys. Rev. D **70**, 105021 (2004).
- [3] J. Greensite, Š. Olejník, and D. Zwanziger, Phys. Rev. D **69**, 074506 (2004); A. Nakamura and T. Saito, Prog. Theor. Phys. **115**, 189 (2006).
- [4] J. R. Finger and J. E. Mandula, Nucl. Phys. **B199**, 168 (1982); S. L. Adler and A. C. Davis, Nucl. Phys. **B244**, 469(1984); R. Alkofer and P. A. Amundsen, Nucl. Phys. **B306**, 305 (1988).
- [5] C. D. Roberts and S. M. Schmidt, Prog. Part. Nucl. Phys. **45**, S1 (2000); R. Alkofer and L. von Smekal, Phys. Rep. **353**, 281 (2001); P. Maris and C. D. Roberts, Int. J. Mod. Phys. E **12**, 297 (2003).k
- [6] R. Alkofer, M. Kloker, A. Krassnigg, and R. F. Wagenbrunn, Phys. Rev. Lett. **96**, 022001 (2006).
- [7] K. Langfeld, R. Alkofer and P. A. Amundsen, Z. Phys. C **42**, 159 (1989).
- [8] R. F. Wagenbrunn and L. Ya. Glozman, hep-ph/0605247, accepted for publication in Phys. Lett. B.
- [9] L. Ya. Glozman, Int. J. Mod. Phys. A **21**, 475 (2006).
- [10] L. Ya. Glozman, A. V. Nefediev, and J. E. F. T. Ribeiro, Phys. Rev. D **72**, 094002 (2005).
- [11] L. Ya. Glozman, Phys. Lett. **B587**, 69 (2004).